SHORT FATIGUE CRACK GROWTH IN NEAR α TITANIUM ALLOYS

A.C. Hollis[+] and C.J. Beevers[*]

The effect of Primary α content on Fatigue Crack initiation/propagation was examined in α + β heat treated IMI 834. Cracks were observed to initiate in primary α grains and propagate with equal ease through both transformed β and primary α. Varying the primary a content between 5% and 25% volume fraction had no significant effect on the cracks propagation resistance of IMI 834.

INTRODUCTION

IMI 834 is the first titanium alloy to offer creep resistance above 600°C. Its composition allows control of the microstructure through heat treatment in the α/β phase field. The prior β grain size in IMI 834 is an average of 100μm and this can be compared with 500-800μm for IMI 829 and 1-2 mm for IMI 685. These variations in prior β grain size and subsequent transformed β product can have significant effects upon the short and long fatigue crack growth behaviour these alloys. This paper reports recent observations on IMI 834 and compares them to IMI 685 and Ti-65s.

+ T & N Technology, Cawston House, Cawston, Rugby, Warwickshire, CV22 7SA, U.K.

* School of Metallurgy & Materials and IRC For High Performance Materials, University of Birmingham, Birmingham, B15 2TT, U.K.

EXPERIMENTAL

Material and Testing Procedure

The alloy has the chemical composition (measured in Wt%) Ti-5.8Al-4.0Sn-3.5Zr-7Nb-0.5Mo-0.35Si-0.06C. The material was supplied as 60mm bar stock, in the heat treated condition, by IMI Titanium Ltd. The heat treatments involved solution treatment in the α/β phase field at a temperature consistent with the required volume per cent primary (5%, 15% and 25%). The bar stock was then oil quenched and aged for two hours at 700°C. The microstructures employed are shown in Figure 1a, 1b, 1c with details of the microstructural sizes and tensile properties shown in Table 1.

TABLE 1 - Microstructural Dimensions and Mechanical Properties of Heat Treated IMI 834

Volume % Primary	Primary α Grain Size μm	Prior β Grain Size μm	0.2% Proof Stress MPa
5	16	120	989*
15	19	60	970*
25	22	46	930*

* Data supplied by IMI Titanium Ltd.

Fatigue testing was carried out in tension-tension on a Dartec servo hydraulic testing machine at 20°C in air. Short crack specimens were of the hour glass design, 5mm x 5mm square sectioned reduced to 4mm x 3mm in the centre section to provide a K_t of 1.03. Specimen surfaces to be monitored were ground, polished and etched. Comparative long crack data was obtained from square sectioned corner notched specimens. An R ratio of 0.1 was employed in all tests and an acetate replication technique was employed to monitor crack initiation and growth. Crack length measurements were recorded from replicas using an optical microscope with a cross wire eye piece.

The Mode I stress intensity solutions employed for short and long cracks were those determined by Pickard (1) for semicircular and corner cracks in tension respectively. An a/c ratio of 1 was observed in all

specimens. This ratio was determined by the post failure examination specimens in the scanning electron microscope (SEM).

RESULTS AND DISCUSSION

Crack Initiation

In order to investigate the effects of microstructure on short fatigue cracks it is necessary to compare results from specimens of different microstructures tested at the same fraction of the 0.2% proof stress. This will ensure the effects of plasticity ahead of the cracks should be similar in each microstructure thus enabling the true crack tip/microstructural interactions to be observed.

The crack initiation site in specimens of the three different microstructures, tested in tension-tension, at σ_{max} = 80% of the 0.2% proof stress, was observed to occur from slip bands in primary grains, shown in Figure 2a. However, in earlier work performed in three point bending on specimens with 15% primary α (2) crack initiation was also observed to occur from slip bands in α colonies, Figure 2b.

Fatigue crack initiation appears to be controlled by the location of a grain or colony at the surface which is favourably orientated to the stress axis to develop slip. This effect has been shown by previous workers to occur in nickel and aluminium alloys (3) (4).

Fatigue Crack Propagation

Figure 3 is an optical micrograph recorded from a replica of a crack in a specimen containing 15% primary. From the figure it is apparent that the crack path is well defined and crack propagation appears to take place on well defined crystallographic planes. These planes have been identified from previous work on titanium alloys to be of the (0001) kind (5).

The rate of growth exhibited by cracks underwent marked changes which were dependent upon the interaction of the crack tip with the local microstructure. This is illustrated in Figures 4a, b and c which are plots of log (da/dn) Vs log (ΔK) for all three microstructures. The scattered nature of the data indicates the crack propagation rates were undergoing periods of acceleration and retardation and even temporary crack arrest, indicated by da/dn = 10^{-8}mm/cycle. The

microstructural features causing temporary arrest were α colonies and primary α grains. Arrests occurring with equal frequency at either feature, in all three microstructures.

Figure 4a, b and c also compare the short and long crack propagation rates in each microstructure. The figures reveal similar trends in all three microstructures, namely the short crack data shows crack growth at ΔK levels below the applied long crack threshold. Also at ΔKs below 10 MPa$\sqrt{m}$ the short crack data falls into a wide scatter band. Above ΔK = 10 MPa$\sqrt{m}$ the scatter in the short crack data is reduced and there is good agreement between the short and long crack data.

Figure 5 compares the short crack data obtained in the investigation to data obtained in other near α alloys IMI 685 (6) and Ti-65s(7). Firstly, it is apparent that all the data for IMI 834 falls into a large scatter band. This suggests that no significant differences in crack propagation resistance occur as a result of varying the volume percent primary α, and thus significantly altering the average prior β grain size (Table 1), in IMI 834. This is in contrast to the work of Wagner et al (8) who working with equiaxed Ti-8.6Al showed short fatigue cracks to propagate faster in a large grained material (100μm) than in a small grained material (20μm). However, Brown and Taylor (9) observed no grain size effect in α/β heat treated Ti-6Al-4V of grain sizes 4.7μm and 11.7μm respectively. This could have been due to the difference in grain sizes being too small to significantly affect the crack propagation resistance. Alternatively the apparent absence of a grain size effect in α/β heat treated alloys could be due to the fact that any effect of microstructure, on these alloys resistance to fatigue crack propagation, is dependent not only upon the α and prior β grain sizes, but also upon the size and orientation of the transformed β product. Therefore, unless there is a significantly large difference in these variables from one structure to the next it will be difficult to observe a grain size effect on crack propagation rates.

Figure 5 compares the crack growth data for IMI 834, Ti-65s and IMI 685, with prior ß grain sizes of 100μm, 1.5mm and 5mm respectively. The figure shows that as the microstructure is refined, in near α alloys, the resistance to fatigue crack propagation is

increased. This observation supports the above suggestion that only when a very large variation in microstructural dimensions occurs will a significant effect on crack propagation resistance be measureable.

CONCLUSIONS

1. Fatigue crack initiation occurs from slip bands in favourably orientated primary α grains or α colonies.

2. Short fatigue crack growth occurs along crystallographic planes in both the primary α grains and α colonies.

3. No effect of primary α content on fatigue crack propagation resistance in IMI 834 was observed when microstructures with 5%, 15% and 25% primary α were examined.

4. A transition from short crack growth to long crack growth appears to occur at a ΔK value of approximately 10 MPa$\sqrt{m}$, in IMI 834.

5. IMI 834 possesses a greater resistance to fatigue crack propagation than either IMI 685 or Ti-65s.

ACKNOWLEDGEMENTS

The authors would like to thank Rolls Royce PLC, in particular, Dr. L. Grabowski for financial support and useful discussions, also the MOD (Pyestock) for financial support.

REFERENCES

1. Pickard, A.C. The Application of 3-D Finite Element Methods to Fracture Mechanics and Fatigue Life Prediction, P. 81, 1986.

2. Hollis, A.C. & Beevers, C.J. Internal Report, EP309555525/2P, May 1989. Birmingham University.

3. Healy, J.C. Private Communication.

4. Mulvihill, P.J. PhD Thesis, Birmingham University, 1986.

5. Ward-Close, C.M. PhD Thesis, Birmingham University, 1978.

6. Brown, C.W. & Hicks, M.A. Fatigue of Engineerng Materials and Structures, 6, 2, 67-76, 1983.

7. Hastings, P.J., Hicks, M.A. & King, J.A. Fatigue 87, (Proc. Conf.) P. 251, 1987.

8. Wagner, L., Gregory, J.K., Gysler, A. & Lötjering, G. Small Fatigue Cracks (Proc. Conf.), pP. 171, 1986.

9. Brown, C.W. & Taylor, D. Fatigue Crack Growth Threshold Concepts (Proc. Conf)., P. 252, 1983.

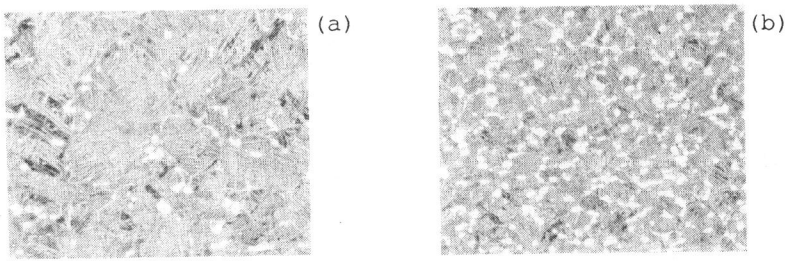

Figure 1. Optical Micrographs of IMI 634 α/β Heat Treated to attain (a) 5%, (b) 15% and (c) 25% Primary α in the Microstructure.

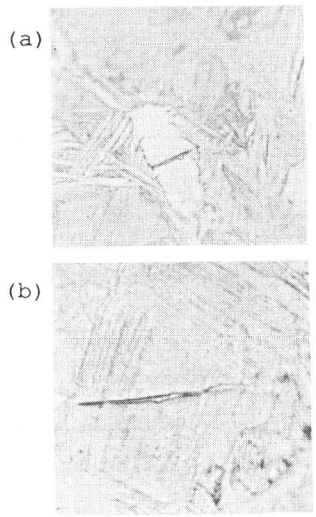

Figure 2. Optical Micrographs of crack Initiation Sites in (a) Primary α grain and (b) α colony.

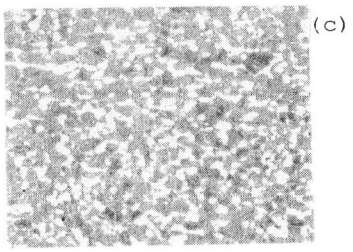

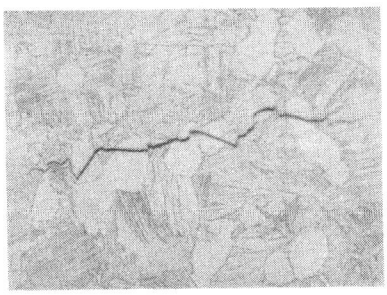

Figure 3. Micrograph of Crack Profile in a Specimen Containing 15% Primary α.

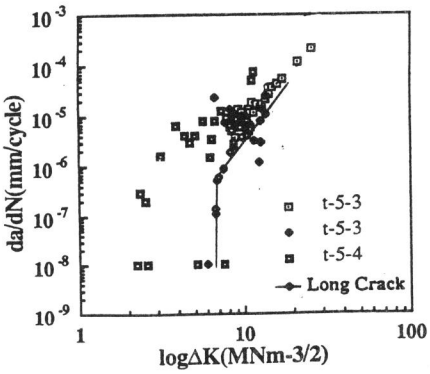

Figure 4a
Fatigue Crack Growth in IMI 834 Containing 5% Primary α.

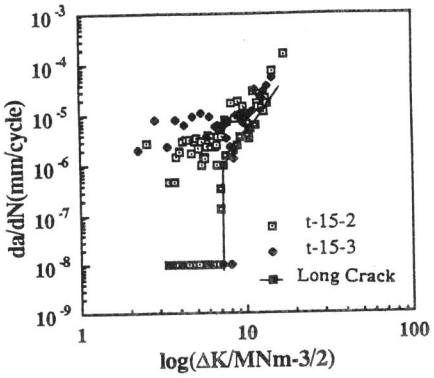

Figure 4b
Fatigue Crack Growth in IMI 834 Containing 15% Primary α.

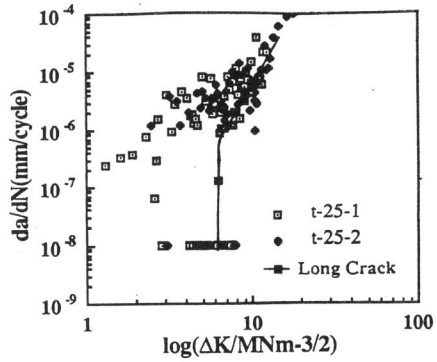

Figure 4c
Fatigue Crack Growth in IMI 834 Containing 25% Primary α.

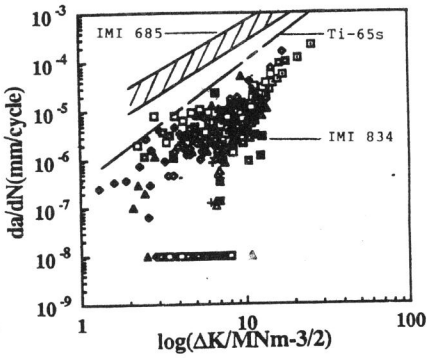

Figure 5
Comparison of Fatigue Crack Growth Data for IMI 834, IMI 685 (6) and Ti-65s (7).